

Scanning Electrochemical Microscopy. 17. Studies of Enzyme-Mediator Kinetics for Membrane- and Surface-Immobilized Glucose Oxidase

David T. Pierce, Patrick R. Unwin,[†] and Allen J. Bard*

Department of Chemistry and Biochemistry, The University of Texas at Austin, Austin, Texas 78712

The scanning electrochemical microscope (SECM) can be used to detect electron-transfer reactions of tip-generated species that occur at nonconductive surfaces containing a redox-active enzyme. Experiments were carried out with glucose oxidase immobilized on several substrates and the apparent kinetics of the enzyme catalysis were measured for several mediator oxidants under conditions of high D-glucose concentration. Theory for the SECM feedback current was developed to model the limiting zero- and first-order electron-transfer kinetics expected for such surface catalysis. Working curves relating the SECM feedback current to surface rate constants are presented. For substrates with glucose oxidase covalently attached to the surface or trapped within a porous membrane, the enzyme reaction was readily detected and the SECM feedback currents measured at low mediator concentration (ca. 50 μM) were found to exclusively fit the model for zero-order heterogeneous kinetics. However, at low enzyme surface concentration or with extensive chemical cross-linking of immobilized glucose oxidase, it was very difficult to use the SECM to detect and quantify the enzyme reaction. General guidelines for studying enzyme surface reactions with the SECM are given, and the prospects for detecting and kinetically assaying enzymes of cellular, and even subcellular, samples are discussed.

INTRODUCTION

A number of diverse applications of the scanning electrochemical microscope (SECM), including imaging and micro-fabrication at the liquid-solid interface, have recently been reviewed.^{1,2} In addition to these uses, the SECM is also capable of probing the kinetics of solution reactions^{3,4} and adsorption phenomena,⁵ as well as monitoring and quantifying heterogeneous electron-transfer kinetics associated with processes on conducting surfaces.^{6,7} In this paper, we demonstrate for the first time that electron-transfer kinetics can also be probed for nonconductive surfaces containing redox-active enzymes. We describe how the SECM can be used to detect redox catalysis exhibited by an immobilized enzyme and present a method to measure the apparent kinetics of the surface-catalyzed electron-transfer reaction. From these results, we discuss the experimental factors which could interfere with detection and kinetic analysis of immobilized

enzymes and assess the prospects for studying and imaging the reactivity of enzyme-containing biological samples with the SECM.

The SECM derives its imaging capability and kinetic sensitivity from the chemical communication, generally referred to as feedback, induced between a substrate surface and a movable ultramicroelectrode (UME) tip. In this well-defined feedback mode,⁸ the UME is held at a potential where electrolysis of a dissolved redox mediator (R) is diffusion-controlled. When the tip is positioned far from a target surface, usually a distance greater than about 10 UME radii, the steady-state current (i_{ss}) depends only upon characteristics of the mediator and the electrode itself (Figure 1a). The surface does not communicate with the tip, and the current is simply defined by the well-known UME equation (eq 1),

$$i_{T,\infty} = 4nFD_Rc_R^*a \quad (1)$$

where c_R^* , D_R , and n are respectively the bulk concentration, diffusion coefficient, and number of electrons in the mediator reaction, a is the electrode radius, and F is the Faraday constant. At closer distances, the surface begins to intercept or impede both redox forms of the mediator. For insulating or nonreactive substrates, the surface blocks R from diffusing to the tip and the steady-state current decreases from $i_{T,\infty}$ (Figure 1b). Currents lower than $i_{T,\infty}$ demonstrate a negative feedback communication between the UME and the surface. For conducting substrates, poised at a potential sufficient to reverse the tip reaction, the surface intercepts the mediator species generated at the tip (O) and regenerates R (Figure 1c). This new source of R within the UME/substrate gap increases the steady-state current from $i_{T,\infty}$. Currents greater than $i_{T,\infty}$ demonstrate a positive feedback communication between the UME and the target substrate.

Clearly, the rate at which the mediator is regenerated on the substrate governs the ultimate SECM feedback response. Previous work has demonstrated the effects of finite substrate electron-transfer kinetics on the SECM response and has shown that rate effects are manifested by currents ranging between the purely positive and purely negative feedback limits.⁶ Recently, theory of the SECM steady-state current has also been developed which accurately models these intermediate feedback currents and allows the heterogeneous electron-transfer kinetics to be quantified.⁷ In general, these studies have shown that the SECM is sensitive to a wide range of heterogeneous rate constants, because the two pure feedback responses often differ by orders of magnitude under typical experimental conditions.

To date, the SECM has been used exclusively to study heterogeneous electron-transfer reactions at conducting surfaces such as metals,⁹ carbon electrodes,⁶ and conducting polymer films.¹⁰ In such studies, the thermodynamic driving

[†] Present address: Department of Chemistry, University of Warwick, Coventry, U.K. CV4 7AL.

(1) Bard, A. J.; Denuault, G.; Lee, C.; Mandler, D.; Wipf, D. O. *Acc. Chem. Res.* 1990, 23, 357.

(2) Bard, A. J.; Fan, F.-R. F.; Pierce, D. T.; Unwin, P. R.; Wipf, D. O.; Zhou, F. *Science* 1991, 254, 68.

(3) Unwin, P. R.; Bard, A. J. *J. Phys. Chem.* 1991, 95, 7814.

(4) Zhou, F.; Unwin, P. R.; Bard, A. J. *J. Phys. Chem.* 1992, 96, 4917.

(5) Unwin, P. R.; Bard, A. J. *J. Phys. Chem.* 1992, 96, 5035.

(6) Wipf, D. O.; Bard, A. J. *J. Electrochem. Soc.* 1991, 138, 469.

(7) Bard, A. J.; Mirkin, M. V.; Unwin, P. R.; Wipf, D. O. *J. Phys. Chem.* 1992, 96, 1861.

(8) Kwak, J.; Bard, A. J. *Anal. Chem.* 1989, 61, 1221.

(9) Kwak, J.; Bard, A. J. *Anal. Chem.* 1989, 61, 1794.

(10) Lee, C.; Bard, A. J. *Anal. Chem.* 1990, 62, 1906.

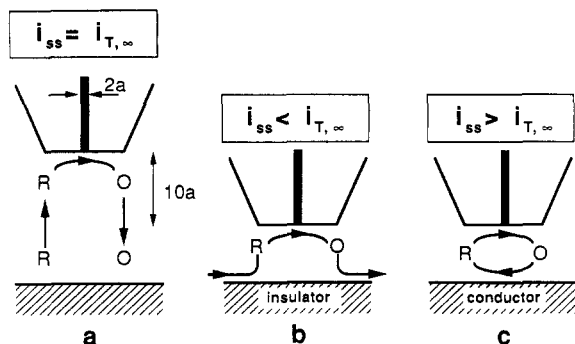


Figure 1. Schematic representing diffusion of an electrolyzed mediator R in the SECM. (a) With the UME far in solution, unhindered diffusion yields the steady-state current, $i_{T,\infty}$. (b) With the UME near an insulating substrate, the diffusion of R is hindered (outer diffusion profile of R, $c_R/c_R^* = 0.95$, in shaded area) and i_{ss} is lower than $i_{T,\infty}$. (c) With the UME near a conductor, the mediator is re-formed and i_{ss} is greater than $i_{T,\infty}$.

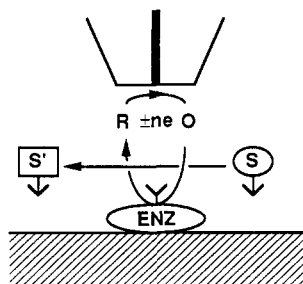
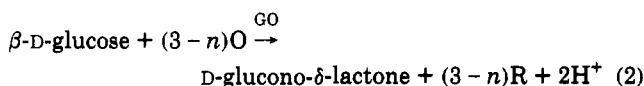


Figure 2. Schematic depicting the principles of SECM feedback detection of an immobilized enzyme (ENZ). With the UME near the surface, the mediator (R) is regenerated in the presence of the enzyme-specific reactant (S).

force for regenerating the tip-produced mediator was electrochemical in nature and, as such, could be varied continuously. However, high substrate conductivity is not a prerequisite for investigating heterogeneous electron-transfer kinetics. In principle, any substrate which can interact chemically with O to reverse the tip reaction (generate R) can influence the SECM feedback response and can be studied for apparent kinetic limitations. In the present work and in a forthcoming paper,¹¹ we demonstrate this principle with substrates containing immobilized electron-transfer enzymes known as oxidoreductases. These enzymes catalyze the transfer of electrons between an electron donor (R) or acceptor (O) and an enzyme-specific reactant molecule (S). As shown in Figure 2, donor or acceptor (mediator) species generated at the SECM tip provide the reducing or oxidizing equivalents (n) that react with S in an enzyme-catalyzed reaction occurring only at the substrate surface. In this mode, the enzyme causes the regeneration of the mediator species, R, consumed at the UME and the rate of the enzyme reaction is directly transduced into current measured by the SECM. Hence, the magnitude of the feedback response depends upon the rate at which the enzyme catalytically regenerates the bulk form of the donor or acceptor. For substrates capable of undergoing high rates of catalysis, the SECM current will demonstrate a positive feedback response. An overall negative feedback response will result from a slow or hindered enzyme reaction which may be larger than that seen over a pure insulator.

In this paper, we report the feedback response of surface- and membrane-immobilized glucose oxidase (GO), a robust enzyme isolated from the mold *Aspergillus niger*. Both as an immobile substance and in solution, GO catalyzes the oxidation of β -D-glucose to D-glucono- δ -lactone by a number

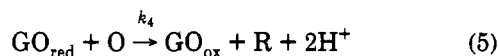
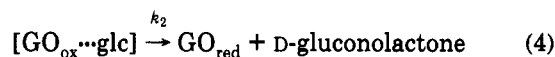
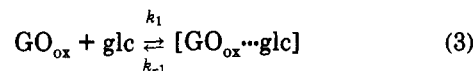
of one- and two-electron mediator oxidants.¹²



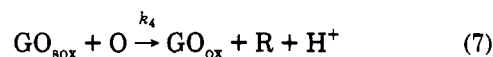
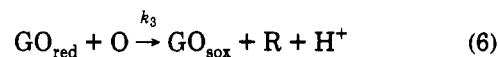
where O represents an n -electron mediator oxidant ($n = 1, 2$). Using surfaces containing artificially immobilized GO, we examine conditions under which the reaction in eq 2 can be detected by the SECM and explore the effect of surface morphology on the feedback current. Using finite-difference methods to theoretically model the SECM response, we quantitatively evaluate the feedback behavior of immobilized GO and assess the apparent heterogeneous kinetics of the catalyzed reaction.

THEORY

Rate Equation for Glucose Oxidase Catalysis. The reaction expressed in eq 2 oversimplifies the mechanism known for catalysis of GO in solution and of GO immobilized on surfaces or membranes. The actual catalytic scheme for both forms of GO is best modeled as an alternating two-reactant or "ping-pong" mechanism^{13,14} where GO is sequentially reduced and the reoxidized within one catalytic cycle. In this process, β -D-glucose (glc) acts to reduce the enzyme while the electron-deficient mediator acts as the oxidant. With two-electron oxidants ($n = 2$), such as the natural acceptor O_2 , conventional steady-state techniques and transient relaxation methods have identified a number of kinetically distinct reactions (eqs 3–5) which involve GO in a solitary



form or as a binary complex, $[\]$.^{13,15–18} For one-electron oxidants ($n = 1$), the mechanism is not as well understood but is presumed¹² to involve the participation of a semioxidized form of the enzyme (GO_{sox}), in addition to the fully reduced and oxidized forms (eqs 3, 4 and 6, 7). For reasons



of simplicity, we have only considered outer-sphere, irreversible electron transfer between reduced GO and the mediator oxidants in eqs 5–7. Since little direct chemical evidence has substantiated enzyme-bound forms of these

(12) Bartlett, P. N.; Tebbutt, P.; Whitaker, R. G. *Prog. React. Kinet.* 1991, 16, 55.

(13) Bight, H. J.; Porter, D. J. T. In *The Enzymes. Volume XII: Oxidation-Reduction, Part B: Electron Transfer(II), Oxygenases, Oxidases(I)*; Boyer, P. D., Ed.; Academic: New York, 1975; Chapter 7.

(14) Carr, P. W.; Bowers, L. D. In *Immobilized Enzymes in Analytical and Clinical Chemistry*; Chemical Analysis, Vol. 56; Elving, P. J., Winefordner, J. D., Kolthoff, I. M., Eds.; John Wiley & Sons: New York, 1980; Chapter 2.

(15) Gibson, Q. H.; Swoboda, B. E. P.; Massey, V. J. *Biochem.* 1964, 239, 3927.

(16) Duke, F. R.; Weibel, M.; Page, D. S.; Bulgrin, V. G.; Luthy, J. J. *Am. Chem. Soc.* 1969, 91, 3804.

(17) Weibel, M. K.; Bright, H. J. *J. Biol. Chem.* 1971, 246, 2734.

(18) Weibel, M. K.; Bright, H. J. *Biochem. J.* 1971, 124, 801.

(11) Pierce, D. T.; Bard, A. J. Unpublished work.

oxidants, we assume no enzyme-oxidant complex intermediates in the present treatment.

A generalized two-reactant rate law for the steady-state consumption (turnover) of both one- and two-electron mediator oxidants can be derived from the rate equations representing eqs 3-7 with a steady-state approximation for the various enzyme forms (i.e., $dc_{GO,ox}/dt = dc_{[GO-glc]}/dt = dc_{GO,red}/dt = 0$). The derivation of this rate equation, shown in eqs 8 and 9, is given in Appendix A. In this rate expression,

$$dc_O/dt = \frac{V_M}{\frac{K_{M,glc}}{c_{glc}} + \frac{K_{M,O}}{c_O} + 1} \quad (8)$$

$$K_{M,glc} = \frac{k_{-1} + k_2}{k_1} \quad K_{M,O} = (2-n)\frac{k_2}{k_3} + \frac{k_2}{k_4}$$

$$V_M = k_{cat}c_{GO,tot} \quad k_{cat} = (3-n)k_2 \quad (9)$$

for $n = 1, 2$

the kinetic constants $K_{M,i}$ reflect the extent to which the enzyme reacts with a particular substrate and the term V_M represents the maximum attainable rate for the catalytic process. Associated with V_M is the total amount of active enzyme in the system ($c_{GO,tot}$) and the efficiency with which the enzyme catalyzes the overall reaction. The rate term defining this efficiency, k_{cat} , is intrinsic to a particular enzyme and the substrates upon which it acts.

Model for Heterogeneous Turnover of Mediator Oxidant. For the purpose of the present treatment, only limiting kinetic cases of the full rate expression (eq 8) are incorporated into the model describing the heterogeneous turnover of mediator oxidant by immobilized GO. These cases assume D-glucose concentrations which greatly exceed the kinetic constant, $K_{M,glc}$. Under conditions of high D-glucose concentration, the full rate equation is simplified to eq 10, which

$$dc_O/dt = \frac{V_M}{\frac{K_{M,O}}{c_O} + 1} \quad c_{glc} \gg K_{M,glc} \quad (10)$$

resembles the well-known Michaelis-Menten expression for one-reactant enzymes.¹⁹⁻²² From this expression, two limiting kinetic cases obtain at large and small mediator oxidant concentrations. These cases, given in eqs 11 and 12, describe

$$dc_O/dt = V_M \quad c_O \gg K_{M,O} \quad (11)$$

$$dc_O/dt = V_M(c_O/K_{M,O}) \quad c_O \ll K_{M,O} \quad (12)$$

the zero-order ($N = 0$) and first-order ($N = 1$) turnover of mediator oxidant, respectively. To incorporate these limiting reaction kinetics into an SECM model for heterogeneous mediator turnover, a geometry for the immobilized enzyme surface is assumed which consists of a porous enzyme layer originating at a level $z = 0$ and extending normal to the surface to a thickness of $z = l$. This layer is considered to be sufficiently thin and permeable so that the concentrations of mediator oxidant and D-glucose are constant throughout the layer. Defined in this manner, the model assumes no partitioning effects or diffusional limitations.

At steady state, the rate of diffusion of mediator oxidant into the layer is equal to its rate of turnover by the enzyme. For the limiting kinetic conditions described in eqs 11 and 12 for mediator turnover, these mass balance relationships are

$$D_O(\partial^2 c_O/\partial z^2) = \partial c_O/\partial t = V_M(c_O/K_{M,O})^N \quad N = 0, 1 \quad (13)$$

where D_O is the diffusion coefficient of the oxidized mediator. Solutions of the mass balance equations and differentiation with respect to the diffusion axis (z)²³ yield flux expressions (J_N) for the mediator oxidant at the enzyme boundary layer ($z = l$) which are directly related to the zero- and first-order heterogeneous rate constants for mediator turnover (k_N) as well as the maximal flux (J_M).

$$D_O(\partial c_O/\partial z) = J_N = J_M(c_O/K_{M,O})^N = k_N(c_O)^N \quad N = 0, 1 \quad (14)$$

$$J_M = k_{cat}lc_{GO,tot} \quad N = 0, 1 \quad (15)$$

Formulation and Solution of the SECM Problem.

Calculation of the SECM feedback current requires the solution of cylindrical diffusion equations for species O and R which are appropriate to the SECM geometry. Boundary conditions for these equations must describe both the substrate geometry and the heterogeneous reaction occurring at the target surface as well as conditions relating to the UME probe, including the axis symmetry and the radial edge of the tip-substrate domain.⁸ The boundary conditions for the N -order ($N = 0$ or 1) heterogeneous reaction of O at the substrate are of the form

$$D_O(\partial c_O/\partial z) = k_N(c_O)^N = -D_R(\partial c_R/\partial z) \quad (16)$$

where $z = d$ and $0 \leq r \leq r_{glass}$, D_i and c_i are respectively the diffusion coefficient and concentration of species i ($i = O$ or R), z and r are the distances normal and radial to the UME, starting at its center, d and r_{glass} denote the tip-substrate separation and the radius of the UME probe (electrode and insulating glass sheath combined), and k_N is the zero- or first-order heterogeneous rate constant. For the steady-state feedback problem, the relevant diffusion equations for both O and R are identical to eq 3 of ref 3 (with $\partial c_i/\partial t = 0$), and the remaining boundary conditions are given by eqs 6-10 of ref 3.

The problem is cast into dimensionless form through the introduction of the normalized variables defined in eqs 11-13 of ref 3 and the normalized heterogeneous rate constant defined as

$$K_N = k_N a / D(c_R^*)^{1-N} \quad (17)$$

where, for simplicity, we take $D = D_O = D_R$. Solutions to the problem were obtained numerically using the alternating-direction implicit (ADI) finite difference method of Peaceman and Rachford.²⁴ Details of the calculation for the specific case of $N = 1$ have been given elsewhere.⁷ Modifications to this procedure, which are required to treat the case of $N = 0$, are described in Appendix B.

Theoretical Results. Typical calculated working curves of normalized UME current, $i_T/i_{T,\infty}$, as a function of normalized heterogeneous rate constant (over a range applicable to the work reported in this paper) are shown in Figure 3a,b for zero- and first-order kinetics, respectively. Curves are presented for a range of normalized tip-substance separations

(19) Ikeda, T.; Miki, K.; Senda, M. *Anal. Sci.* 1988, 4, 133.

(20) Parker, J. W.; Schwartz, L. S. *Biotechnol. Bioeng.* 1987, 30, 724.

(21) Atkinson, B.; Lester, D. E. *Biotechnol. Bioeng.* 1974, 16, 1299.

(22) Yokoyama, K.; Tamiya, E.; Karube, I. *J. Electroanal. Chem. Interfacial Electrochem.* 1989, 273, 107.

(23) Blaedel, W. J.; Kissel, T. R.; Boguslaski, R. C. *Anal. Chem.* 1972, 44, 2030.

(24) Peaceman, D. W.; Rachford, H. H. *J. Soc. Ind. Appl. Methods* 1955, 3, 28.

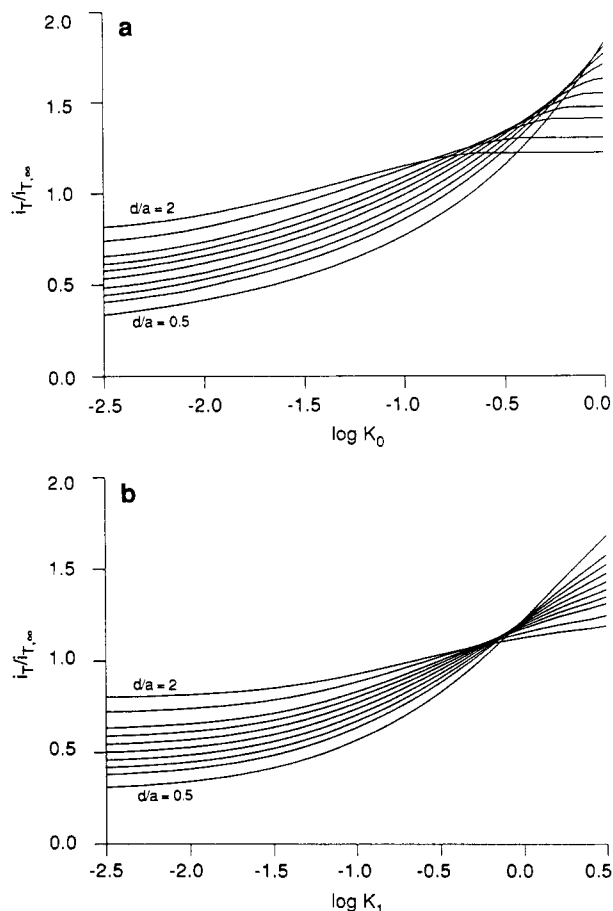


Figure 3. Steady-state working curves relating normalized tip current to the (a) zero- and (b) first-order normalized heterogeneous rate constant K_N . Curves in ascending order on the ordinate axis correspond to normalized tip-substrate distances $\log(d/a)$ of $-0.3, -0.2, -0.15, -0.1, -0.05, 0.0, 0.05, 0.1, 0.2, \text{ and } 0.3$, respectively.

and all curves relate to a UME probe with $RG = r_{\text{glass}}/a = 10$. The curves are in accord with qualitative expectations. For small d/a (e.g., 0.5, bottom curves), when the rate is small, an overall negative feedback is observed because blocking of diffusion to the tip by the substrate is more important than the regeneration reaction. However, even in this situation, the normalized current at the tip is larger than that for a purely insulating substrate ($K_N \rightarrow 0$). For larger values of K_N , positive feedback is observed. The same effects are observed, but are greatly attenuated, at larger distances between the tip and substrate (e.g., $d/a = 2$).

An important point in these theoretical results is the extent to which the SECM feedback measurements can discriminate between zero- and first-order heterogeneous processes. From the forms of the working curves in Figure 3a,b, resolution of the two mechanistic cases should be possible using SECM current-distance measurements, provided that the normalized kinetic parameter falls within the faster kinetic domain of the data presented (e.g., $\log K_N \geq -1.0$). If the (normalized) kinetics are relatively slow, approaching pure negative feedback behavior over an insulator (i.e., $\log K_N < -2.5$), the similarity of the i_T versus d working curves would not allow a distinction between the two cases.

EXPERIMENTAL SECTION

Materials. All solutions were prepared with 18-M Ω Milli-Q reagent water (Millipore Corp.). Buffer solutions used for enzyme assays and substrate storage were prepared from 0.1 M K_2HPO_4 (Baker Analyzed) and 70% $HClO_4$ (analytical reagent, Mallinckrodt, Inc.) with the precise pH measured with an Orion Model 91-05 glass membrane electrode and Model 701A meter. For use

as redox mediators in SECM experiments, ferrocenecarboxylic acid (FcCOOH; 97%, Aldrich), methyl viologen dichloride ($MVCl_2$, 98%, Aldrich), potassium ferrocyanide ($[K_4][Fe(CN)_6]$; ACS reagent, MCB Manufacturing Chemists Inc., Norwood, OH), and hydroquinone (H_2Q ; 99+%, Aldrich) were used as received. α -D-Glucose (ACS reagent, Aldrich) was used as a precursor to the enzyme-specific reactant, β -D-glucose (glc), and was used as received. Solutions containing D-glucose were prepared at least 24 h before each experiment and stored at room temperature to allow complete equilibration of the α - and β -anomers. For the fabrication of enzyme substrates, Nylon 66 (Al Plastics, Austin, TX), triethyloxonium tetrafluoroborate (TOTFB; 0.1 M in CH_2Cl_2 , Fluka), 1,4-diaminobutane (DAB; 98%, Aldrich), glutaraldehyde (GA; 25% in water, Polysciences), (γ -aminopropyl)-triethoxysilane (PCR Research), 2-propanol (Baker analyzed), poly(ethylene glycol) diglycidyl ether (PEG 400; Polysciences), bovine serum albumin (BSA; 98–99%, Sigma), and glucose oxidase (GO, EC 1.1.3.4; type X from *A. niger*, 125 IU mg^{-1} , 186 000 $g \text{ mol}^{-1}$, Sigma) were used as received. All solutions used to analyze enzyme kinetics were deoxygenated with humidified Ar.

Electrochemical Apparatus. Solubilized-enzyme kinetic measurements and diffusion coefficient measurements of redox mediators were performed using an all-glass small-volume cell (0.1–0.5 mL) with a glassy-carbon working disk ($r_{\text{disk}} = 1.57 \text{ mm}$, Bioanalytical Systems, West Lafayette, IN), a platinum counter electrode, and a silver quasi-reference electrode (AgQRE) placed in the assay solution. A purge-gas inlet allowed deoxygenation of the assay solution. Cell potential and current measurement were controlled by a Bioanalytical Systems Model 100B electrochemical analyzer.

Immobilized-enzyme kinetic measurements were performed with a scanning electrochemical microscope (SECM) similar in design to that described previously.⁹ The two-electrode cell used in SECM experiments (1–2 mL) was machined from Teflon and equipped with a AgQRE and a drilled plastic cap which allowed access for the tip UME and an Ar purge tube. A recessed Teflon bottom with an O-ring seal was threaded into the base of the cell to allow easy mounting of both square- and disk-shaped substrates. The carbon tip UMEs used in all experiments were fabricated by heat-sealing 8- μ m-diameter carbon fibers (AVCARB CF125G, Type 84, Textron Specialty Materials, Lowell, MA) in 2-mm-o.d. Pyrex tubes under vacuum. The electrochemical radius of each electrode was $4.0 \pm 0.5 \mu\text{m}$, as measured from the diffusion-limited cathodic current of the $[Ru(NH_3)_6]^{3+/2+}$ couple in 0.1 M pH 7.0 phosphate buffer,²⁵ and the optically measured glass radius (r_{glass}) was either 10 ± 2 or 20 ± 2 times the carbon fiber radius. A final polishing of the UME tip was performed before each experiment with 0.05- μ m alumina.

The potential of the tip UME was poised with a Princeton Applied Research Corp. (PARC, Princeton, NJ) Model 173 potentiostat and Model 175 voltage programmer. The counter electrode lead was shorted to the AgQRE and the currents generated at the tip were measured with a home-built preamplifier (gain, 10^4 ; RC, 10 ms) placed in series with a PARC Model 179 current-to-voltage converter. With this configuration and proper electronic shielding, currents as small as $\pm 2 \text{ pA}$ could be reliably measured. No precautions were made to thermostat the SECM cell during experiments which were all performed at ambient temperature (22–25 $^\circ\text{C}$).

Enzyme Substrates. GO substrates were prepared for SECM analysis having three distinct enzyme environments. In most cases, enzyme substrates were analyzed within 24 h of fabrication.

Form I. Covalent Immobilization on Nylon. Immobilization of GO on Nylon 66 disks was carried out by a modified O-alkylation procedure of Morris et al.^{26,27} During enzyme coupling, the treated surface turned a pink color which did not intensify with higher enzyme solution concentrations or longer coupling times. From enzyme binding data reported by Thompson et

(25) The diffusion coefficient for $[Ru(NH_3)_6]^{3+}$ in 0.1 M pH 7.0 phosphate buffer was taken as $5.48 \times 10^{-6} \text{ cm}^2 \text{ s}^{-1}$ as given by: Bauer, J. E.; Wightman, R. M. *J. Electroanal. Chem. Interfacial Electrochem.* 1991, 305, 73.

(26) Morris, D. L.; Campbell, J.; Hornby, W. E. *Biochem. J.* 1975, 147, 593.

(27) Thompson, R. Q.; Mandoke, C. S.; Womack, J. P. *Anal. Lett.* 1985, 18, (B1), 93.

al.,²⁷ the GO surface concentration of these maximally coupled samples was estimated to be 3.4×10^{-10} mol cm⁻². In some cases, the enzyme-coupling time was shortened to decrease the amount of bound GO. Treated disks were stored in phosphate/perchlorate buffer (pH 7.0) at 4 °C.

Form II. Immobilization in Hydrogel Membranes. The procedure used to form GO membranes was similar to that outlined by Heller and co-workers for GO hydrogel films immobilized on carbon electrodes.^{28,29} Aqueous 20 wt % solutions of BSA, GO, and PEG-400 were added to the surfaces of aminated glass slides³⁰ with the volume ratios (45 - x):x:5 μ L ($0 \leq x \leq 25$ μ L), respectively. After the solutions were mixed thoroughly, each slide was spun at 500 or 1000 rpm on a Model 1-EC10-R485 photoresist spinner (Headway Research Inc., Garland, TX) until the adhering liquid was evaporated (ca. 5 min). These cast slides were cured at 35 °C for 48 h, washed with water, and stored in phosphate/perchlorate buffer (pH 7.0) at 4 °C. Profilometry (Alpha-step Model 100, Tencor Instruments, Mountain View, CA) showed membrane thicknesses of 1.0 ± 0.1 and 0.05 ± 0.01 μ m for slides cast at 500 and 1000 rpm, respectively. The average density of cured 50 wt % GO hydrogel fragments was 1.43 ± 0.04 g cm⁻³ (by weight of known volumes of density-matched aqueous ZnCl₂ solutions). From these properties, the surface concentrations of GO in 50 wt % hydrogel membranes were estimated to be 4.0×10^{-10} and 2.0×10^{-11} mol cm⁻² for thick and thin films, respectively.

Form III. Immobilization in Langmuir-Blodgett (LB) Films. The immobilization of GO in compact LB films has been described by Sun et al.³¹ Films were similarly prepared at room temperature on cleaned (piranha solution) glass microscope slides (0.2 \times 1.3 \times 1.3 cm) with a Lauda film balance and film lift (Brinkman Instrument Co., Westbury, NY). Transfer coefficients of GO (1.2 ± 0.3) indicated approximate monolayer coverage with each lift cycle. Assuming ideal monolayer transfer, the surface concentration of GO per monolayer was calculated to be 1.8×10^{-13} mol cm⁻² using a measured surface area per GO molecule of 900 ± 100 Å². Immobilized films of 1-5 monolayers were allowed to dry at room temperature and then immediately analyzed.

SECM Enzyme Assay Procedure. GO catalysis at prepared surfaces was monitored from phosphate/perchlorate buffer solutions (pH 7.0) containing two redox mediators and the enzyme-specific reactant, β -D-glucose. The two mediators served separate functions as electron acceptor from immobilized GO and as calibrant of the tip-substrate distance. Because it does not interfere with the GO catalysis, the methyl viologen 2+/+ couple was used for distance calibration in all experiments, whereas the ferrocenecarboxylic acid 0/+ , the ferrocyanide 4-/3- , or the H₂Q/Q couples were separately employed to mediate the GO surface reaction (i.e., to serve as R/O, Figure 2). SECM experiments were generally performed by the following procedure. After the assay solution was thoroughly deoxygenated in the SECM cell, the UME tip was first poised at a potential where the diffusion-controlled reduction of MV²⁺ was maintained and the tip was translated toward the surface (z-axis, 0.5 μ m s⁻¹). Translation was stopped when the steady-state current for the reduction of MV²⁺ decreased to less than $0.5i_{T,\infty}$. The pure negative feedback response of this couple provided a direct estimate of the tip-substrate distance.⁸ Without alteration of the UME position, a potential sufficient to irreversibly oxidize the second mediator was applied to the tip and the electrode was translated away from the surface (z-axis, 100 nm s⁻¹). Current and distance were recorded at each 0.1 μ m during translation. After the distance calibration provided by the MV^{2+/+} couple was applied, i_T versus d curves were made dimensionless by dividing d by the tip electrode radius (a) and i_T by the unperturbed steady-state

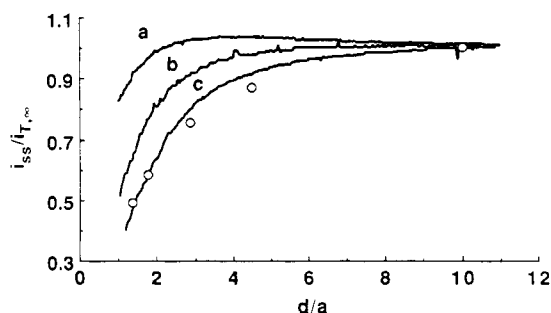


Figure 4. Normalized current-distance curves recorded for the mediator, 0.5 mM FcCOOH, in 0.1 M pH 7.0 phosphate/perchlorate buffer with 50 mM D-glucose. With the tip near Nylon surfaces bound with GO (substrate form I), curves a and b correspond to surfaces with maximum and less than maximum bound GO, respectively. Curve c was obtained with the maximum bound GO and no D-glucose in the assay solution. Circles denote the theoretical current-distance behavior for an insulating (nonreactive) substrate. The UME tip RG was 20 in all curves.

current ($i_{T,\infty}$). In most cases, the i_T versus d curves obtained for all enzyme substrates were reproducible within ± 5 -10% over the range of feedback-sensitive tip-substrate distances. Reproducibility between identically prepared substrates was usually better than ± 10 %.

EXPERIMENTAL RESULTS AND DISCUSSION

SECM Detection of GO Surface Catalysis. Three enzyme-immobilized surfaces having quite different interfacial morphologies and enzyme environments (forms I-III in Experimental Section) were fabricated and tested for catalytic reactivity by the SECM.

Figure 4 shows the steady-state currents obtained for GO covalently bound to Nylon (form I) for $0 < d/a \leq 10$. With ferrocenecarboxylic acid (FcCOOH) acting as mediator and with no β -D-glucose in solution, the tip currents measured by the SECM demonstrated only negative feedback behavior at all tip-substrate distances (curve c). An identical response was also obtained when no GO was coupled to the Nylon surface and D-glucose was present in the assay solution. As anticipated, the tip currents in both cases agreed within experimental error to currents predicted for insulating or nonreactive surfaces (circles). In contrast to this behavior, assay solutions containing a high concentration of D-glucose (50 mM) with substrates having the maximum amount of GO coupled to the Nylon yielded tip currents for the FcCOOH mediator which demonstrated a small, but well-defined, positive feedback (curve a). At intermediate distances, $2 \leq d/a \leq 8$, these positive feedback currents increased as the tip-substrate distance decreased. Only at $d/a \leq 2$ did the tip currents begin to decrease and demonstrate a negative feedback character. Feedback response of this type resembled the current-distance behavior observed for slow electron transfer at electrode substrates⁶ and demonstrated that the redox catalysis of immobilized GO could augment the SECM tip current. Detectable GO catalysis was also observed when smaller amounts of GO were coupled to the Nylon surface (curve b). In this case, however, the tip currents were significantly reduced from the maximal response in curve a and demonstrated a predominantly negative feedback character.

Hydrogel substrates had more rigorously controlled enzyme concentrations and environments than those on Nylon and were prepared by chemically cross-linking bovine serum albumin (BSA) and GO to form a highly porous membrane. These hydrogen membranes (form II) generally showed catalytic responses with the SECM which were similar to the Nylon-bound GO. Figure 5 shows i_T - d curves for 50 wt % GO membranes obtained with the FcCOOH mediator in assay solutions containing 50 mM D-glucose. In curves a and b, the

(28) Gregg, B. A.; Heller, A. *J. Phys. Chem.* 1991, 95, 5976.

(29) Pishko, M. V.; Michael, A. C.; Heller, A. *Anal. Chem.* 1991, 63, 2268.

(30) Cut glass microscope slides (0.2 \times 1.3 \times 1.3 cm) were cleaned in 1:4 H₂O₂ (30%)/concentrated H₂SO₄ (piranha solution—CAUTION!) and aminated in a boiling 4:1:1 wt % solution of 2-propanol, water, and (γ -aminopropyl)triethoxysilane. This treatment is similar to a method for binding thiol functional groups to glass surfaces described by: Goss, C. A.; Charych, D. H.; Majda, M. *Anal. Chem.* 1991, 63, 85.

(31) Sun, S.; Ho-Si, P.-H.; Harrison, D. *J. Langmuir* 1991, 7, 727.

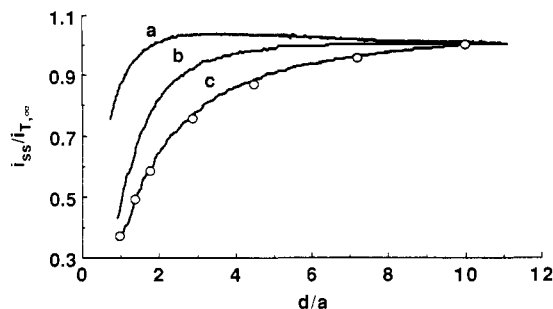


Figure 5. Normalized current-distance curves recorded for the mediator, 0.5 mM FcCOOH, in 0.1 M pH 7.0 phosphate/perchlorate buffer with 50 mM D-glucose. With the tip near 50 wt % GO hydrogel membranes (substrate form II), curves a and b correspond to 1.0- and 0.05- μm -thick membranes, respectively. Curve c corresponds to a 1.0- μm -thick membrane which has been excessively treated with PEG. Circles denote the theoretical current-distance behavior for an insulating (nonreactive) substrate. The UME tip RG was 10 for curves a and b. Tip RG was 20 for curve c and theory.

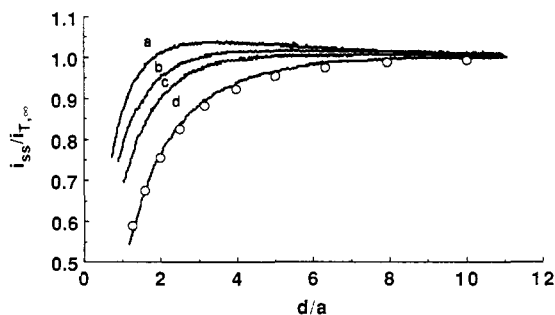


Figure 6. Normalized current-distance curves recorded for the mediator, 0.5 mM FcCOOH, in 0.1 M pH 7.0 phosphate/perchlorate buffer with 50 mM D-glucose. With the tip near 50 wt % GO hydrogel membranes (substrate form II), curves a-d correspond to 1.0- μm -thick membranes composed of 50, 5, 1, and 0 wt % GO, respectively. Circles denote the theoretical current-distance behavior for an insulating (nonreactive) substrate. The UME tip RG was 10 in all curves.

steady-state currents were appreciably larger than the theoretically predicted insulator response (circles). However, the membrane thickness for the substrate of curve a was approximately 20 times greater than that in curve b. This direct relation between the amount of catalytic feedback current and membrane thickness indicated a low resistance of the hydrogel matrix to mediator and D-glucose diffusion. If the oxidized mediator or the D-glucose reactant had not been able to penetrate the matrix and reach GO sites within the membrane, the feedback responses of the two films would have been comparable. Since the tip currents for the thicker film were greater than those of the thinner film, the mediator and D-glucose were clearly able to penetrate into the membrane on the time scale of the SECM experiment.

As with the Nylon substrates, feedback response of the hydrogel membranes also depended on the amount of bound GO. Figure 6 shows the i_T - d curves (a)-(d) for thick hydrogel membranes composed of 50, 5, 1, and 0 wt % GO, respectively. For hydrogel membranes containing no bound GO, the SECM response closely fit the theory for an insulating substrate (circles). With increasing GO content, the tip current response showed an increasing positive feedback contribution which was consistent with an enzyme-controlled rate of mediator turnover.

A final effect tested with the hydrogel substrates was the influence of excess diepoxide (PEG) cross-linking of the albumin-GO matrix. After a thick membrane of 50 wt % GO composition was fabricated and cured, the sample was soaked in a solution of 20% PEG for 1 h, air dried, and recured. The resulting sample demonstrated only the pure negative feed-

back predicted for insulating substrates (Figure 5c). Although deactivation of the enzyme may have occurred because of chemical modification of active prosthetic sites on individual GO molecules, the excess cross-linking probably also inhibited diffusion within the membrane and thereby slowed the catalytic reaction. These internal diffusion limitations are frequently encountered in immobilized enzyme systems and have received considerable attention.³²

The final form of immobilized GO tested for catalytic reactivity by the SECM was a cross-linked derivative of native GO assembled in Langmuir-Blodgett (LB) monolayers (form III). The derivatization of the native GO involved intramolecular cross-linking with the dialdehyde, glutaraldehyde, which added rigidity to the protein structure surrounding GO and rendered the GO molecule more amenable to assembly in LB films.^{31,33} Although films up to five GO monolayers were tested for enzymatic reactivity using the SECM, none produced feedback currents with the FcCOOH mediator and high D-glucose concentrations which were significantly different from the pure insulator response. To see if allosteric effects related to cross-linking limited the SECM response, the homogeneous catalysis rates of native and cross-linked GO were tested electrochemically using the method described by Cass et al.³⁴ Comparing the results of both enzyme forms, the cross-linked GO was found to have lost only 25% of the original reactivity exhibited by the native enzyme. This relative kinetic indifference to cross-linking has been observed in other studies with solubilized GO^{31,33} which employed standard enzymatic techniques. Since the inability to observe any catalytic reactivity of GO LB films by the SECM was probably not due to cross-linking effects, it was possible that diffusional resistances within the compact LB assemblies or low surface concentrations of assembled GO influenced the SECM response. Calculations using the area per molecule measured for the cross-linked GO showed that the surface concentration of GO in the LB films was approximately 1.8×10^{-13} mol cm^{-2} per monolayer. This concentration, even for the five monolayer films, was more than 1 order of magnitude lower than the surface concentration of 2×10^{-11} mol cm^{-2} estimated for GO in the thin 50 wt % GO hydrogel membranes. Since the thin hydrogel membranes showed only limited catalytic response by the SECM (Figure 5b), the GO LB films probably showed no apparent catalytic reactivity because of low enzyme surface concentration.

A final point to be noted in the present qualitative treatment regards the inability of the SECM to detect monolayer coverage of immobilized GO in LB films and the significant reactivity observed for GO bound to Nylon disks. If the enzyme was bound only to the Nylon surface in the form I substrates, the GO LB findings indicate that no reactivity should have been observed. Since considerable enzyme reactivity was observed (Figure 4), more GO must have been bound to the Nylon than could have been present at the disk-solution interface. This finding has some support from the quantitative GO-binding data reported by Thompson et al.²⁷ which indicate that the GO surface concentration in the form I substrates (3.4×10^{-10} mol cm^{-2}) far exceeds monolayer coverage (ca. 10^{-13} mol cm^{-2}). In light of the relatively smooth appearance of these substrates at the micron level, the chemical procedure used to immobilize GO on Nylon probably disrupted the Nylon surface at a submicron level and allowed

(32) Engasser, J.-M.; Horvath, C. In *Immobilized Enzyme Principles*; Applied Biochemistry and Bioengineering, Vol. 1; Wingard, L. B., Jr., Katchalski-Katzir, E., Goldstein, L., Eds.; Academic: New York, 1976; p 127.

(33) Solomon, B.; Lotan, N.; Katchalski-Katzir, E. *Biopolymers* 1976, 16, 1837.

(34) Cass, A. E. G.; Davis, G.; Francis, G. D.; Hill, H. A. O.; Aston, W. J.; Higgins, I. J.; Plotkin, E. V.; Scott, L. D. L.; Turner, A. P. F. *Anal. Chem.* 1984, 56, 667.

Table I. Average Apparent Rate Constants^a for Zero- and First-Order Heterogeneous Glucose Oxidase Catalysis Measured at High D-Glucose Concentration^b

mediator, R ^c	[R]/mM	zero order		first order	
		10 ¹¹ k' ₀ /mol cm ⁻² s ⁻¹	% RSD	10 ³ k' ₁ / cm s ⁻¹	% RSD
FcCOOH	0.05	5.14	11.3	5.54	53.7
	0.50	39.9	15.0	3.57	13.3
	2.0	<i>d</i>		<i>d</i>	
[Fe(CN) ₆] ⁴⁻	0.05	5.85	8.2	7.16	65.3
	0.50	2.44	18.5	0.16	23.8
	2.0	<i>e</i>		<i>e</i>	
H ₂ Q	0.02	5.25	11.3	52.3	53.2
	0.05	5.58	11.5	6.14	49.0
	0.50	12.4	10.0	1.10	28.0
	2.0	18.9	27.0	0.35	39.4

^a Normalized rate constants (K_N) at $\log(d/a) = -0.15$ to $+0.3$ were determined from normalized SECM currents using the working curves in Figure 3a,b. Average apparent rate constants ($k'_N = K_N D_R [R]^{1-N}/a$) and percent relative standard deviations (% RSD) for each $\log(d/a)$ set are reported. ^b Experimental conditions: (UME tip) $a = 4.0 \mu\text{m}$, $RG = 10$; (assay solution) mediator and 50 mM D-glucose in 0.1 M pH 7.0 phosphate/perchlorate buffer; (substrate) form II, 50 wt % GO, $l = 1.0 \pm 0.1 \mu\text{m}$, $[\text{GO}] = 4.0 \times 10^{-10} \text{ mol cm}^{-2}$. ^c Diffusion coefficients of mediators (D_R) measured in the assay solution (note b) were $6.40 \times 10^{-6} \text{ cm}^2 \text{ s}^{-1}$ (FcCOOH), $6.19 \times 10^{-6} \text{ cm}^2 \text{ s}^{-1}$ ([Fe(CN)₆]⁴⁻), and $7.76 \times 10^{-6} \text{ cm}^2 \text{ s}^{-1}$ (H₂Q). ^d FcCOOH was not completely soluble at this concentration. ^e Feedback currents were too small for analysis, $\log(K'_N) < -2.5$.

the enzyme to bind within a thin, porous, membrane- or fractal-like structure. The similarity between SECM responses (Figures 4 and 6) and GO surface concentrations (ca. $10^{-10} \text{ mol cm}^{-2}$) of the Nylon and the thick hydrogel substrates also seems to support some type of microporous Nylon surface structure.

Kinetic Analysis of the GO Surface Catalysis. To measure the finite kinetics of the GO surface catalysis described in eqs 3–7, steady-state SECM feedback experiments were carried out on identical 50 wt % GO hydrogel substrates (form II) using a wide range of bulk concentrations (usually 50 μM to 2.0 mM) of three different mediator couples. In all of these experiments, the concentration of D-glucose was kept at the high level of 50 mM to ensure that the simplified rate expressions for the GO surface reaction (eqs 11 and 12) remained valid at all times. This saturating level of D-glucose was consistent with apparent kinetic constants of $K'_{M,glc} \leq 10 \text{ mM}$ frequently reported for gel-immobilized GO.^{35–38} The i_T - d curves obtained for each assay solution were analyzed using both the zero- and first-order working curves in Figure 3a,b, respectively. In most cases, normalized tip currents of an experimental curve were used to calculate apparent rate constants (k'_N) for each d/a in Figure 3, and the set of values was averaged to yield a mean rate constant and a standard deviation across the range of d/a . These average observed zero- and first-order rate constants are listed in Table I for the various mediator conditions employed.

The most striking feature of the the kinetic data in Table I is the clear discrimination of zero-order behavior at the lowest mediator concentrations (20–50 μM). For each of the FcCOOH, [Fe(CN)₆]⁴⁻, and H₂Q mediators, the relative standard deviations (RSD) of the first-order rate constants for the range of d/a were consistently greater than 50%, while the RSD for the zero-order rate constants were typically less than 12%. A more informative illustration of this reaction

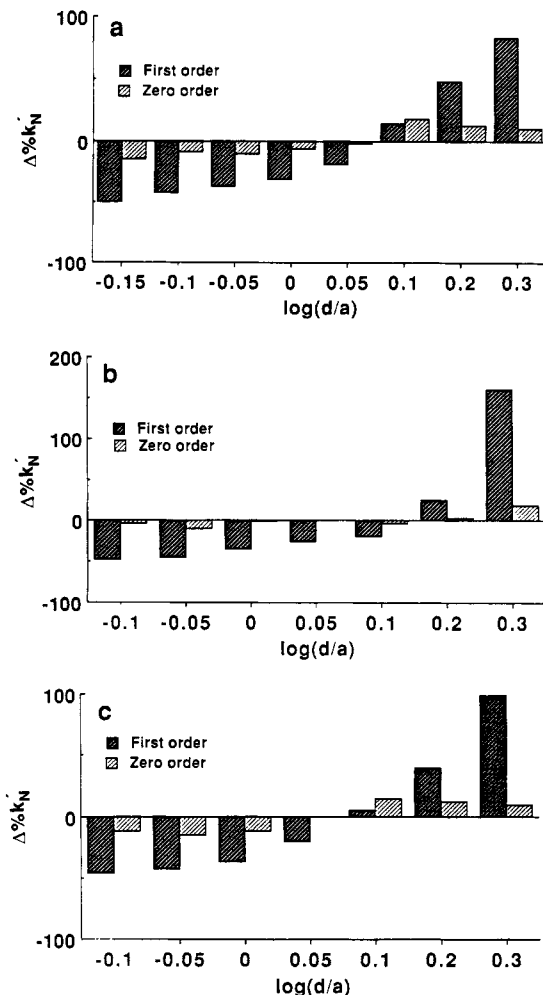


Figure 7. Percent deviations from average zero- and first-order heterogeneous rate constants measured for the 0.05 mM mediators (a) FcCOOH, (b) [Fe(CN)₆]⁴⁻, and (c) H₂Q at various normalized distances (d/a) from a 50 wt % GO hydrogel membrane (substrate form II, membrane thickness 1.0 μm).

order discrimination is shown in Figure 7, where the percent deviation of each rate constant from the average is displayed at each of the analyzed tip-substrate distances. At the farthest of the analyzed distances, the first-order deviations from average were greatest and ranged from more than 50% for the FcCOOH and H₂Q mediators, to more than 150% for the [Fe(CN)₆]⁴⁻ mediator. Such extreme deviations were not observed for the zero-order rate constants, which demonstrated no significant systematic variation from the average and were all within $\pm 20\%$ of the mean. At somewhat higher concentrations, the zero-order rate constants determined for the H₂Q and [Fe(CN)₆]⁴⁻ mediators also seemed to fit the measured tip currents better. In both cases, deviations of the first-order rate constants over the range of tip-substrate distances were consistently greater than deviations of the zero-order rate constants, often by a factor of 3 or more, and the first-order deviations suffered from the same positive trend observed at the lowest mediator concentrations. In addition, over the wide range of concentrations studied, both mediators showed much better correspondence for zero-order rate constants, while first-order analysis yielded rate constants which varied by over 2 orders of magnitude. Although this behavior strongly suggests that surface catalysis and mediator turnover by GO in the hydrogel membranes were limited by zero-order processes, it should be noted that at the highest mediator concentrations, where $\log K_N$ was less than -1 , discrimination between zero- and first-order kinetics became difficult.

(35) Shu, F. R.; Wilson, G. S. *Anal. Chem.* 1976, 48, 1679.

(36) Castner, J. F.; Wingard, L. B., Jr. *Biochemistry* 1984, 23, 2203.

(37) Kimura, J.; Saito, A.; Ito, N.; Nakamoto, S.; Kuriyama, T. *J. Membr. Sci.* 1989, 43, 291.

(38) Gregg, B. A.; Heller, A. *Anal. Chem.* 1990, 62, 258.

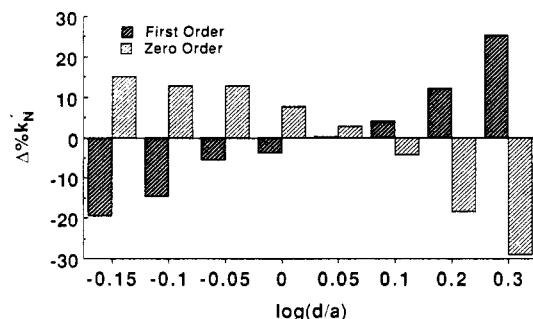


Figure 8. Percent deviations from average zero- and first-order heterogeneous rate constants measured for 0.5 mM FcCOOH at various normalized distances (d/a) from a 50 wt % GO hydrogel membrane (substrate form II, membrane thickness 1.0 μm).

Since the data in Table I demonstrated a clear discrimination of zero-order mediator turnover for most experimental conditions, the observed zero-order rate constants, as expected, were also essentially independent of the form of the mediator. Such behavior was consistent with saturating conditions of both enzyme reactants and, as related in eq 12, indicated that the observed zero-order rate constants in Table I were equivalent to an apparent maximal heterogeneous turnover rate, J'_M . From eq 15 and the known GO surface concentration of the 50 wt % membranes (4.0×10^{-10} mol cm^{-2}), the apparent turnover rate of the immobilized enzyme (k'_{cat}) was calculated for each mediator, yielding an average observed rate of 0.15 s^{-1} . This value of k'_{cat} was more than 3 orders of magnitude lower than the intrinsic value (k_{cat}) reported by Weibel and Bright^{17,18} for solubilized as well as immobilized GO. Although a small maximal turnover may have resulted in our system from significant deactivation of GO during immobilization in the hydrogel membranes, our data are not sufficiently detailed to assess this discrepancy.

A final point to be noted in this quantitative treatment is the one exception to zero-order behavior observed for the FcCOOH mediator at high concentration (0.5 mM in Table I). Under these experimental conditions, the relative standard deviations of both the zero- and first-order rate constants were nearly equivalent and both limiting cases demonstrated considerable systematic deviations over the range of d/a . Interestingly, the systematic trend in the the first-order rate constants was nearly equal and opposite to the trend in the zero-order rate constants (Figure 8). Such behavior was indicative of a mixed kinetic regime in which a first-order process begins to limit the GO catalysis with increasing mediator concentration. Since the pseudo-one-substrate model for GO catalysis (eq 10) should only demonstrate a zero- to first-order transition with decreasing mediator concentration, another first-order process is necessary to explain the anomalous FcCOOH behavior. One possibility might be a limitation in the diffusion of the oxidized mediator into the hydrogel membrane. However, the complex kinetic treatment necessary to model coupled diffusion and reaction processes²³ is beyond the scope of this paper.

Assaying Enzymes of Biological Samples. The feedback method presented for assaying GO should be generally applicable to other biochemically important oxidoreductase enzymes when characteristics of the enzyme surface and the SECM system are carefully matched. This match can be achieved by considering how SECM detection is dependent upon enzyme- or substrate-dependent factors as well as parameters controlled in the SECM experiment. For zero-order conditions, where the heterogeneous rate observed by the SECM (k_0) is at its maximum and is equivalent to the maximal mediator flux (J_M), the practical limits of the working curves in Figure 3a demonstrate that zero-order surface catalysis cannot be readily discerned at normalized rate

constants less than 10^{-3} . From eqs 15 and 17 and under the assumption of this lower limit for K_0 , a enzyme detection criteria for the SECM can be conveniently expressed as

$$k_{\text{cat}} l c_{\text{enz,tot}} = J_M \approx k_0 \geq 10^{-3} D_R c_R / a \quad (18)$$

where c_R is the concentration of mediator species consumed at the UME tip and a is the UME radius. From this criterion, enzymatic detection by the SECM can be improved either by reducing the combined experimental parameters on the right side of eq 18 or by increasing the net enzyme/surface factors on the left side of the equation. The preceding analysis of GO reactivity has demonstrated how enzyme/surface factors, namely the enzyme layer thickness and total concentration, can be altered to influence SECM response to the catalyzed reaction. However, for the analysis of natural enzyme samples, it is often not practical or possible to alter the enzyme or its matrix to improve SECM detection. In these cases, only the mediator concentration and the UME probe radius can be appreciably changed to improve detection and possible quantitation of the target enzyme.

The SECM feedback method presented in this paper allows the kinetic reactivity of immobilized enzymes to be studied under a number of practicable conditions. In most cases, the immobilized enzymes can be probed from solutions which closely approximate the pH and ionic strength conditions under which the native enzyme operates. Also, it is possible to quantify the localized redox catalysis associated with enzymes immobilized on insulating surfaces or materials such as biomembranes. Finally, enzyme sites, by virtue of their specific reactivity, can be spatially resolved over small surface areas using the lateral scanning ability of the SECM. This factor has not been fully exploited in the present study, but it has been demonstrated previously by Wang et al.³⁹ and will be more critically addressed in a forthcoming paper.¹¹ Some caution, however, should be exercised when applications that may require high spatial resolution are considered. Spatial resolution of the SECM is governed by the diameter of the UME tip² which can be fabricated, with some difficulty, to as small as 0.1 μm or below.^{40,41} However, changing the size of the UME tip can influence enzyme detection by the SECM, as indicated in eq 18, and reducing the tip radius can make reactivity discrimination more difficult. With presently available SECM apparatus and the feedback techniques described in this work, it appears possible to detect enzyme surface reactions occurring over micron-sized regions.^{2,11} This level of spatial resolution should allow ready enzymatic analysis of cellular-sized bodies and, with some difficulty, should permit investigations of some subcellular organelles.

CONCLUSIONS

The present study has demonstrated the ability of the SECM to detect the redox catalysis occurring at a variety of nonconductive surfaces containing the immobilized oxidoreductase enzyme glucose oxidase. The method developed for detecting the surface reaction relies on the feedback communication between the immobilized enzyme and the SECM tip through the use of a freely diffusing redox mediator. The apparent steady-state kinetics of the GO catalysis were measured under conditions of high D-glucose concentration using theory developed for the SECM current. We are currently applying the feedback methodology described herein to study redox reactions of biological substrates in situ and

(39) Wang, J.; Wu, L.-H.; Li, R. *J. Electroanal. Chem. Interfacial Electrochem.* 1989, 272, 285.

(40) Lee, C.; Miller, C. J.; Bard, A. J. *Anal. Chem.* 1991, 63, 78.

(41) Fan, F.-R. Unpublished experiments.

testing the spatial resolving power of the SECM for mapping enzymatic reactivity at the micron level.

ACKNOWLEDGMENT

We gratefully thank Ling Ye, Tim O'Hara, Yaw Obeng, and David Wipf for helpful advice and discussions. The support of this research by grants from the Robert A. Welch Foundation and the National Science Foundation is gratefully acknowledged. P.R.U. thanks the SERC for the award of a NATO fellowship.

APPENDIX A

We derive a general rate expression (eq 8) which describes the mechanism for consumption of one- or two-electron mediator oxidants by reduced glucose oxidase.

For two-electron mediator oxidants (eqs 3-5), the following material balance and steady-state conditions hold for the various forms of GO.

$$c_{GO,tot} = c_{GO,ox} + c_{[GO\cdots glc]} + c_{GO,red} \quad (A1)$$

$$dc_{GO,ox}/dt = dc_{[GO\cdots glc]}/dt = dc_{GO,red}/dt = 0 \quad (A2)$$

From the rate laws for eqs 3 and 4

$$dc_{[GO\cdots glc]}/dt = k_1 c_{GO,ox} c_{glc} - (k_{-1} + k_2) c_{[GO\cdots glc]} = 0 \quad (A3)$$

the concentration of glucose-bound is given by rearrangement

$$c_{[GO\cdots glc]} = \frac{k_1}{k_{-1} + k_2} c_{GO,ox} c_{glc} \quad (A4)$$

Concentrations of the fully reduced and fully oxidized enzyme are found in a similar fashion as

$$c_{GO,red} = \frac{k_1}{k_{-1} + k_2} \frac{k_2}{k_4} \frac{c_{GO,ox} c_{glc}}{c_O} \quad (A5)$$

$$c_{GO,ox} = \frac{c_{GO,tot}}{1 + \frac{k_1}{k_{-1} + k_2} \frac{k_2}{k_4} \frac{c_{glc}}{c_O} + \frac{k_1}{k_{-1} + k_2} c_{glc}} \quad (A6)$$

From the rate law for consumption of the two-electron mediator oxidant

$$dc_O/dt = k_4 c_{GO,red} c_O \quad (A7)$$

substitution of $c_{GO,red}$ and $c_{GO,ox}$ yields the final rate equation (A8) for the case of two-electron oxidants.

$$dc_O/dt = \frac{k_2 c_{GO,tot}}{\frac{k_{-1} + k_2}{k_1} \frac{1}{c_{glc}} + \frac{k_2}{k_4} \frac{1}{c_O} + 1} \quad (A8)$$

For the mechanistic scheme involving one-electron mediator oxidants (eqs 3, 4, 6, and 7), the material balance of enzyme is

$$c_{GO,tot} = c_{GO,ox} + c_{[GO\cdots glc]} + c_{GO,red} + c_{GO,sox} \quad (A9)$$

and, for conditions of steady state, the concentrations of each enzyme form are

$$c_{[GO\cdots glc]} = \frac{k_1}{k_{-1} + k_2} c_{GO,ox} c_{glc} \quad (A10)$$

$$c_{GO,red} = \frac{k_1}{k_{-1} + k_2} \frac{k_2}{k_3} \frac{c_{GO,ox} c_{glc}}{c_O} \quad (A11)$$

$$c_{GO,sox} = \frac{k_3}{k_4} c_{GO,red} = \frac{k_1}{k_{-1} + k_2} \frac{k_2}{k_4} \frac{c_{GO,ox} c_{glc}}{c_O} \quad (A12)$$

$$c_{GO,ox} = \frac{c_{GO,tot}}{1 + \frac{k_1}{k_{-1} + k_2} \left(\frac{k_2}{k_3} + \frac{k_2}{k_4} \right) \frac{c_{glc}}{c_O} + \frac{k_1}{k_{-1} + k_2} c_{glc}} \quad (A13)$$

From the rate law for consumption of the one-electron mediator oxidant

$$dc_O/dt = k_3 c_{GO,red} c_O + k_4 c_{GO,sox} c_O = 2k_3 c_{GO,red} c_O \quad (A14)$$

substitution of $c_{GO,red}$ and $c_{GO,ox}$ yields the final rate equation (A15) for the case of one-electron mediators.

$$dc_O/dt = \frac{2k_2 c_{GO,tot}}{\frac{k_{-1} + k_2}{k_1} \frac{1}{c_{glc}} + \left(\frac{k_2}{k_3} + \frac{k_2}{k_4} \right) \frac{1}{c_O} + 1} \quad (A15)$$

Finally, a generalized rate equation for cases of one- ($n = 1$) and two-electron ($n = 2$) mediator oxidants (eq 8) is obtained from eqs A8 and A15 by using the substitutions noted in eq 9.

$$dc_O/dt = \frac{V_M}{\frac{K_{M,glc}}{c_{glc}} + \frac{K_{M,O}}{c_O} + 1} \quad (8)$$

$$K_{M,glc} = \frac{k_{-1} + k_2}{k_1} \quad K_{M,O} = (2 - n) \frac{k_2}{k_3} + \frac{k_2}{k_4}$$

$$V_M = k_{cat} c_{GO,tot} \quad k_{cat} = (3 - n) k_2 \quad (9)$$

for $n = 1, 2$

APPENDIX B

A general description of the application of the ADI finite difference method to the solution of SECM problems has been given elsewhere,³ and additional details for the treatment of the feedback mode with first-order irreversible regeneration kinetics at the substrate have also been provided.⁷ Here we describe the necessary changes to the computational method required to treat zero-order (irreversible) surface regeneration kinetics.

Under conditions of equal diffusion coefficients of the participating species, the following mass conservation equation applies (over all space):

$$c_R + c_O = c_R^* \quad (B1)$$

which allows the problem to be condensed to the treatment of one species (in this case R). For the defined steady-state feedback problem, the formal adoption of eq 16 as the surface boundary condition changes the following terms in the calculation from those for first-order heterogeneous kinetics,⁷ where the notation can be understood by referring to ref 3:

$$d_{j,NZ-1} (0 \leq j \leq NE + NG - 2) = [1 - \lambda_Z]CR_{j,NZ-1} + \lambda_Z CR_{j,NZ-2} + \lambda_Z K_0 \Delta Z \quad (B2)$$

$$d_{NE+NG-1,NZ-1} = [1 - \lambda_Z]CR_{j,NZ-1} + \lambda_Z CR_{j,NZ-2} + \lambda_Z K_0 \Delta Z + \lambda_\rho (NE+NG-1) \left\{ 1 + \frac{\Delta \rho}{2} \left[1 + \frac{\exp(-ml\Delta\rho)}{s + m - m \exp(-ml\Delta\rho)} \right] \right\} \quad (B3)$$

$$b_{NZ-1}^{**} (0 \leq j \leq NE + NG - 1) = 1 + \lambda_Z \quad (B4)$$

$$d_{NZ-1}^* (j = 0) = \{1 - 2\lambda_\rho(0)\}CR_{0,NZ-1}^* + 2\lambda_\rho(0)CR_{1,NZ-1}^* + \lambda_Z K_0 \Delta Z \quad (B5)$$

$$d_{NZ-1}^* (1 \leq j \leq NE + NG - 1) = \lambda_\rho(j) \left\{ 1 - \frac{\Delta \rho}{2} \left[1 + \frac{\exp(-ml\Delta\rho)}{s + m - m \exp(-ml\Delta\rho)} \right] \right\} \times CR_{j-1,k}^* + [1 - 2\lambda_\rho(j)]CR_{j,k}^* + \lambda_\rho(j) \left\{ 1 + \frac{\Delta \rho}{2} \left[1 + \frac{\exp(-ml\Delta\rho)}{s + m - m \exp(-ml\Delta\rho)} \right] \right\} CR_{j+1,k}^* + \lambda_Z K_0 \Delta Z \quad (B6)$$

Since the solution of the steady-state feedback problem via the ADI method proceeds in an iterative fashion,⁷ generally from an initial condition appropriate to potential step chronoamperometry, it is necessary to include additional conditions for the treatment of the zero-order problem to ensure that mass is conserved during the iterative process. These are derived from conditions for diffusion-controlled feedback and restrict the maximum rate of the zero-order process to be diffusion-controlled (in R). Thus during the first half-time step of the ADI calculation, the following terms replace those defined above, if $CR_{j,NZ-1} + K_0 \Delta Z > 1$ (defined in double precision)

$$d_{j,NZ-1} (0 \leq j \leq NE + NG - 2) = [1 - 2\lambda_Z]CR_{j,NZ-1} + \lambda_Z CR_{j,NZ-2} + \lambda_Z \quad (B7)$$

$$d_{NE+NG-1,NZ-1} = [1 - 2\lambda_Z]CR_{j,NZ-1} + \lambda_Z CR_{j,NZ-2} + \lambda_Z + \lambda_\rho (NE+NG-1) \left\{ 1 + \frac{\Delta \rho}{2} \left[1 + \frac{\exp(-ml\Delta\rho)}{s + m - m \exp(-ml\Delta\rho)} \right] \right\} \quad (B8)$$

and during the second half-time step, if $CR_{j,NZ-1}^* + K_0 \Delta Z > 1$

$$b_{NZ-1}^{**} (0 \leq j \leq NE + NG - 1) = 1 + 2\lambda_Z \quad (B9)$$

$$d_{NZ-1}^* (j = 0) = \{1 - 2\lambda_\rho(0)\}CR_{0,NZ-1}^* + 2\lambda_\rho(0)CR_{1,NZ-1}^* + \lambda_Z \quad (B10)$$

$$d_{NZ-1}^* (1 \leq j \leq NE + NG - 1) = \lambda_\rho(j) \left\{ 1 - \frac{\Delta \rho}{2} \left[1 + \frac{\exp(-ml\Delta\rho)}{s + m - m \exp(-ml\Delta\rho)} \right] \right\} \times CR_{j-1,NZ-1}^* + [1 - 2\lambda_\rho(j)]CR_{j,NZ-1}^* + \lambda_\rho(j) \left\{ 1 + \frac{\Delta \rho}{2} \left[1 + \frac{\exp(-ml\Delta\rho)}{s + m - m \exp(-ml\Delta\rho)} \right] \right\} CR_{j+1,NZ-1}^* + \lambda_Z \quad (B11)$$

Through this approach it was possible to generate converged working curves, such as those shown in Figure 3b comprising 51 points each, typically in about 1-h CPU time on a VAX 6410 mainframe computer.

RECEIVED for review February 28, 1992. Accepted May 21, 1992.

Registry No. Glc, 50-99-7; FcCOOH, 1271-42-7; ferrocyanide, 13408-63-4; hydroquinone, 123-31-9.